Characterization of deamidation of barstar using electrospray ionization quadrupole time-of-flight mass spectrometry, which stabilizes an equilibrium unfolding intermediate

Santosh Kumar Jha, Putchen Dakshinamoorthy Deepalakshmi,* and Jayant B. Udgaonkar*

National Centre for Biological Sciences, Tata Institute of Fundamental Research, Bangalore 560065, India

Received 19 October 2011; Revised 1 February 2012; Accepted 13 February 2012
DOI: 10.1002/pro.2047
Published online 17 February 2012 proteinscience.org

Abstract: Deamidation of asparaginyl residues is a common posttranslational modification in proteins and has been studied extensively because of its important biological effects, such as those on enzymatic activity, protein folding, and proteolytic degradation. However, characterization of the sites of deamidation of a protein has been a difficult analytical problem. In this study, mass spectrometry has been used as an analytical tool to characterize the deamidation of barstar, an RNAse inhibitor. Upon incubation of the protein at alkaline pH for 5 h, intact mass analysis of barstar, using electrospray ionization quadrupole time-of-flight mass spectrometry (ESI QToF MS), indicated an increase in the mass of +2 Da, suggesting possible deamidation of the protein. The sites of deamidation have been identified using the conventional bottom-up approach using a capillary liquid chromatography connected on line to an ESI QToF mass spectrometer and top down approach by direct infusion of the intact protein and fragmenting inside MS. These chemical modifications are shown to lead to stabilization of an unfolding intermediate, which can be observed in equilibrium unfolding studies.

Keywords: ESI QToF MS; deamidation; peptide sequencing; top down sequencing; protein unfolding; intermediate state

Introduction

Proteins are the work horses in all the living systems. A protein needs to fold into a specific tertiary structure to perform its cellular functions. The primary amino acid sequence of a protein codes for its functional three-dimensional structure,[1–5] but the mechanism of this transfer of information from one dimension to three dimension is poorly understood.[3,4,6,7] In particular, the role of intermediate states during protein folding and unfolding reactions is open to vigorous debate.[8,9] It has been postulated,[10,11] and has also been experimentally shown for many proteins,[12–14] that unfolded protein molecules fold via a sequence of defined events, with the population of various intermediate states, to reach the unique native state. The entropic cost of folding is compensated for, in discrete steps. Intermediate states also serve as useful milestones for describing a protein folding reaction. Recent observations, however, have shown that a few proteins fold in an apparently two-state manner, without accumulation

Santosh Kumar Jha and Putchen Dakshinamoorthy Deepalakshmi contributed equally to this work.

Santosh Kumar Jha's current address is Department of Chemistry, Stanford University, Stanford, California 94305.

Grant sponsors: Tata Institute of Fundamental Research; Department of Biotechnology; Government of India.

*Correspondence to: Jayant B. Udgaonkar, National Centre for Biological Sciences, Tata Institute of Fundamental Research, Bellary Road, Bangalore 560065, India. E-mail: jayant@ncbs.res.in or Putchen Dakshinamoorthy Deepalakshmi, Indian Institute of Science, Bangalore, India. E-mail: pddeepalakshmi@gmail.com

of any detectable intermediate states. The absence of stable intermediates for some proteins has brought into question the relevance of intermediate states during folding and unfolding.[8,15] The confusion is compounded by the fact that for many of these apparently two-state folding proteins, intermediate states could be detected by a change in the folding conditions[16] or by mutagenesis of the protein sequence[17–19] or by using a more sensitive detection method to probe the folding reaction.[20–22] Identifying and populating intermediate states during folding and unfolding,[23] as well as subsequent characterization of their kinetic role,[24] remain a major goal in protein folding studies.

Deamidation of glutamyl and asparaginyl residues is an important nonenzymatic post-translational modification of proteins and peptides. It plays a significant role in various biological processes *in vivo*. Deamidation of β-crystallins can disrupt normal protein–protein interaction and could lead to cataract formation in eyes.[25] It may also affect the immune recognition of proteins and peptides.[26] It has been documented that T cells specifically recognize peptides in which asparagine residues have been deamidated to aspartic acid.[27] It has also been suggested that *in vivo* deamidation of proteins could serve as a molecular timer of many important biological events,[28,29] such as aging.[30–32]

Deamidation of proteins has also been studied extensively *in vitro* because of its effect on the activities of enzymes,[33–36] proteolytic degradation,[37,38] and degradation of protein pharmaceuticals such as immunoglobulin gamma antibodies.[39] The effect of deamidation on the folding reaction of proteins has also been studied in a few cases.[40,41] However, progress in this area has been hampered because the identification and the characterization of the sites of deamidation in a protein has been a difficult analytical problem.[42]

Mass spectrometry (MS) can serve as a very good technique to identify and characterize the sites of deamidation in a protein. Modern mass spectrometers can accurately and precisely measure a mass change of +1 Da, which occur as a result of the $-NH_2 \rightarrow -OH$ chemical modification that occurs during a deamidation reaction.[42–44] In this work, we have used the power of electrospray ionization quadrupole time-of-flight mass spectrometry (ESI QToF MS) to identify and characterize the sites of deamidation in a small protein barstar (Fig. 1) using multiple approaches—bottom-up and top-down sequencing. The effect of deamidation on the folding landscape of barstar has also been investigated.

Barstar is a bacterial protein, and its folding and unfolding reactions have been widely studied.[45–48] No equilibrium intermediates are detected when the folding reaction is measured by probes of global structural change.[17,49] However, the use of high-resolution probes[50] to study its equilibrium unfolding and the effect of a single-site mutation in the protein sequence on its folding[17] have suggested that high-energy intermediate forms might be present at equilibrium during unfolding.[17]

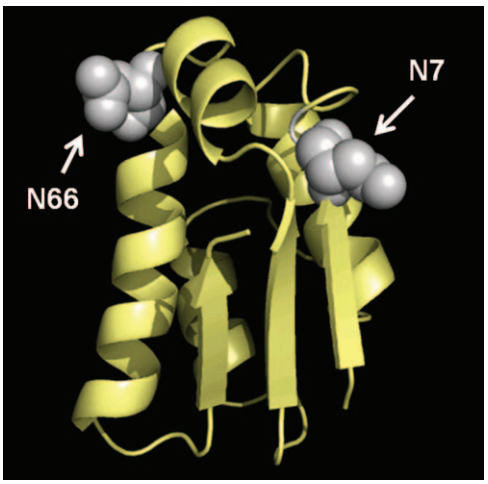

Figure 1. Structure of barstar. The location of deamidation sites, N7 and N66, is shown in gray. The structure was drawn from PDB file 1A19 using the program PyMOL (http://www.pymol.org). [Color figure can be viewed in the online issue, which is available at wileyonlinelibrary.com.]

In this work, we have characterized the deamidation reaction of barstar, which occurs when the protein is incubated at high alkaline pH for few hours, using MS. It is observed that the protein gets deamidated at two out of nine possible deamidation sites. Biophysical characterization of the deamidated protein at pH 8.0 indicates that multiple deamidation reactions do not change the global structure of the protein. Equilibrium unfolding studies on the deamidated protein suggest that deamidation of the protein chain leads to the stabilization of at least one equilibrium intermediate during its unfolding.

Results

The average mass of barstar increases by 2 Da upon incubation at pH 12.5 for 5 h

Figure 2 shows the ESI MS of barstar incubated at pH 12.5 for 0, 2, and 5 h. The observed average mass of WT barstar is 10342.66 Da when the protein was directly infused into ESI QTOF MS [Fig. 2(a)]. The average mass of the protein shifts by +1 Da (10343.62) after 2 h of incubation and by +2 Da (10344.42 Da) after 5 h of incubation at pH 12.5 [Fig. 2(a)]. Figure 2(b) shows the change in the isotopic pattern of eighth charge state of barstar, indicating mass shift upon incubation of the protein at pH 12.5 for 2 and 5 h. Additional change in mass was not observed upon prolonged incubation at pH 12.5 longer than 5 h. The 2 Da increase in the mass of the protein suggests that some chemical modification has occurred in the protein. The observation that the mass increases in steps of 1 Da suggests that this modification could be deamidation of the

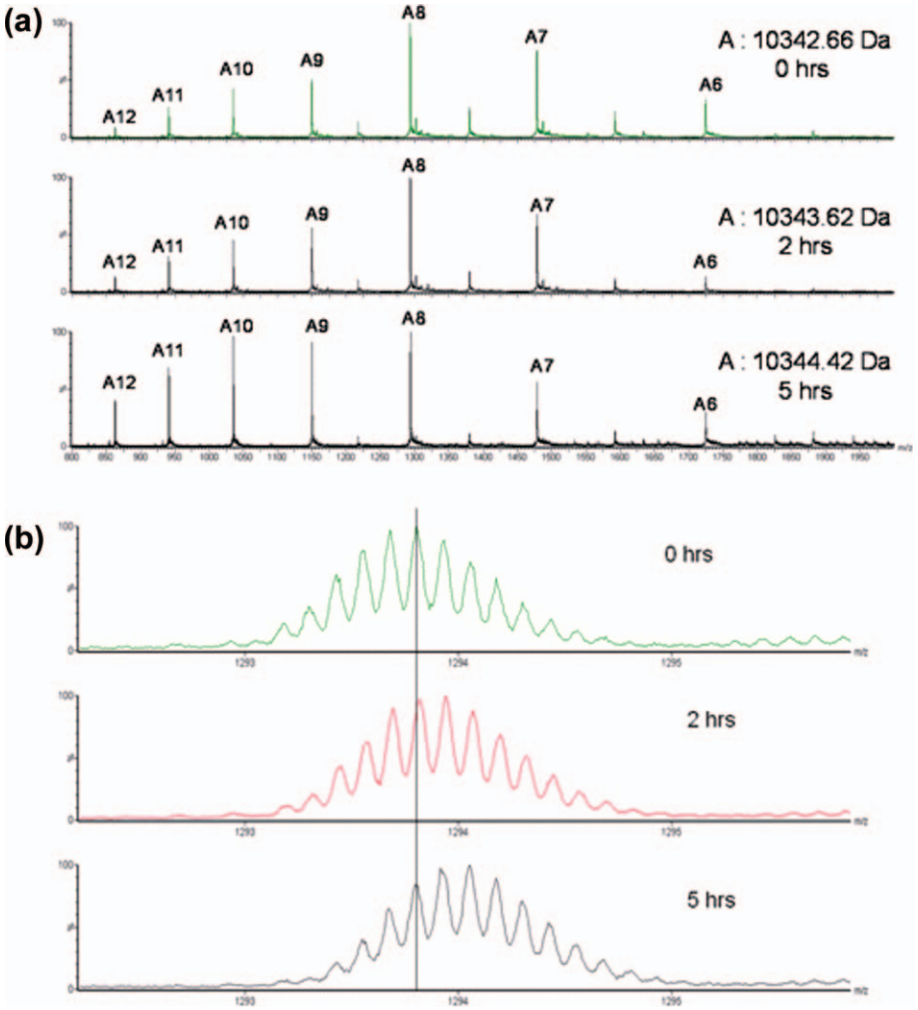

Figure 2. ESI-MS of barstar upon incubation at alkaline pH for different times. (a) The average mass of the protein was measured to be 10342.66, 10343.62, and 10344.42 Da after incubation of the protein at pH 12.5 for 0, 2, and 5 h, respectively. Monomer and noncovalent dimer of barstar were observed under the experimental conditions studied. (b) Changes in eighth charge state of barstar ($[M+8H]^{8+}$) after incubation of the protein at pH 12.5 for 0, 2, and 5 h. The vertical straight line is drawn to guide the eye. The mass spectra were acquired at an instrument resolution of 20,000 (FWHM). [Color figure can be viewed in the online issue, which is available at wileyonlinelibrary.com.]

protein chain (http://www.abrf.org). Apart from the mass of the protein, a noncovalent dimer of the protein is also observed. This indicates that the noncovalent interactions were preserved under the conditions (high concentration of the protein) used, as was observed in an earlier study.[51]

ESI MS analysis of tryptic digest of barstar identifies the modified peptides

To establish that the observed chemical modification is the deamidation of the protein and to find out its site-specific location in the protein chain, the potential sites of deamidation of barstar were determined. The amino acid sequence of barstar, as given in Scheme 1, indicates that there are nine possible sites (three asparagine and six glutamine residues). To identify the possible deamidation sites, barstar was first incubated for different times at pH 12.5 and then reduced, alkylated, and digested with trypsin in a bottom-up approach and injected into the CapLC ESI-MS. Figure 3(a) shows the MS of the tryptic digest of the protein [peptide mass fingerprinting (PMF) data]. The observed PMF data were compared with the theoretical digest of barstar (Table I), generated with 0 missed cleavage of trypsin. The charges on the peptides ranged from 1^+ to 2^+.

MKKAVI**N**GE**Q** IRSISDLH**Q**T LKKELALPEY YGE**N**LDALWD

CLTGWVEYPL VLEWR**Q**FE**Q**S K**Q**LTE**N**GAES VL**Q**VFREAKA

EGCDITIILS

Theoretical Average Mass : 10342.78 Da

Scheme 1. Theoretical sequence of barstar and its potential sites of deamidation. Asparagine residues are shown in bold and underlined and glutamine residues are shown in bold.

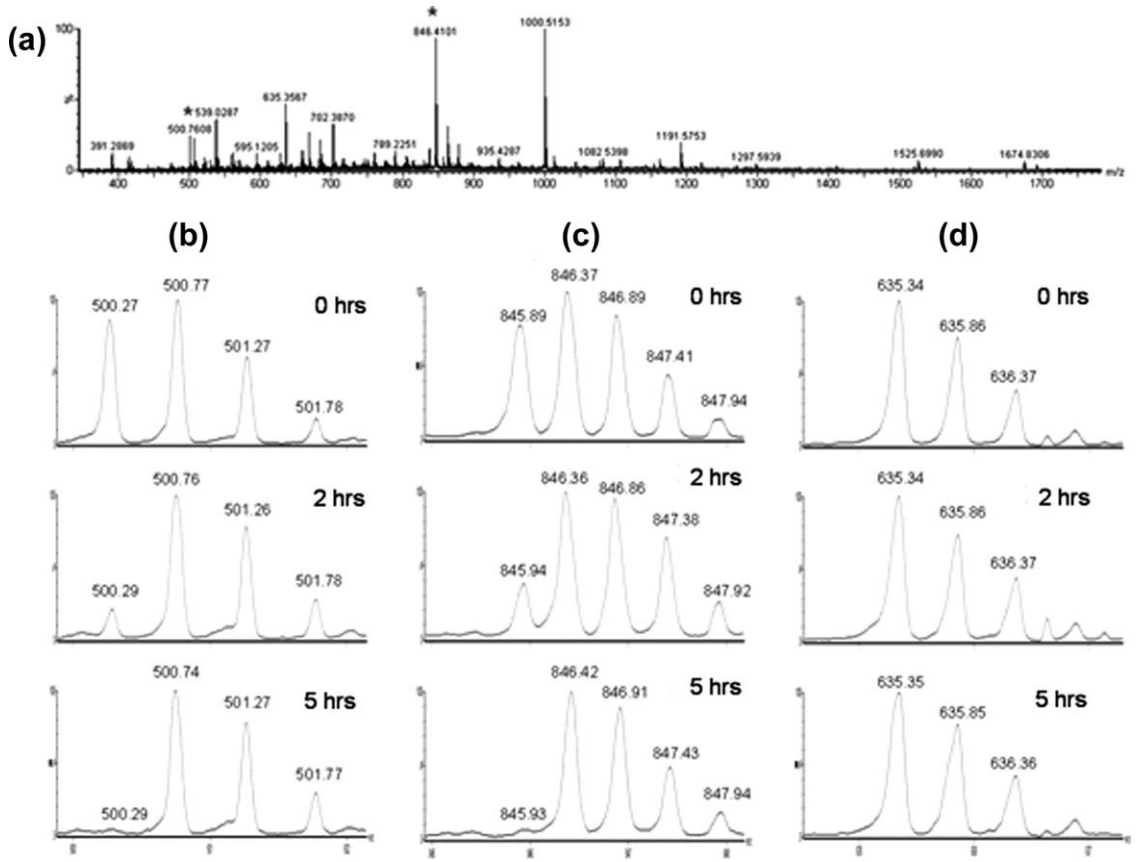

Figure 3. CapLC ESI QToF MS of barstar digested with trypsin overnight at 37°C. (a) PMF of the digested protein has been shown ranging from 350 to 1800 *m/z*.* indicates the peptide T3 and T8 (see Table I). Changes in the isotopic peak distribution of peptides undergoing chemical modification upon incubation at pH 12.5 for various time points. (b) MS of a doubly charged modified peptide (peptide T3) with a mass of 500.27 *m/z*. After 2 h of incubation, the monoisotopic peak intensity is reduced and after 5 h of incubation, the monoisotopic peak has shifted to 500.74 *m/z*. (c) MS of another doubly charged peptide (peptide T8) with a mass of 845.89 *m/z* at different time points of incubation at pH 12.5. The peak shift from 845.89 to 846.42 *m/z* occurs after 5 h of incubation. (d) MS of a control peptide (peptide T4-5, 635.36 *m/z*) whose mass does not change when the protein is incubated at pH 12.5 for different times (0, 2, and 5 h).

Out of the 10 peptides generated (0 missed cleavages), four peptides (T1, T2, T5, and T9) ranged below 500 *m/z*. Two peptides (T9 and T10) did not have the potential deamidation site and one large peptide T6 (1929.69 *m/z*, 2^+), which has a potential deamidation site, was not observed. In addition to these peptides, peptides generated due to missed cleavages were also observed.

Out of the four peptides T3, T4, T7, and T8, each of which contains a possible site of deamidation, only T3 and T8 showed an increase in mass of 1 Da each upon incubation at pH 12.5 for 5 h. Figure 3(b,c) shows that upon incubation at pH 12.5 for 0, 2, and 5 h, the isotopic pattern of peptide T3 (500.28 *m/z*, 2^+) and peptide T8 (845.94 *m/z*, 2^+) changed continuously, resulting in an increase in

Table I. *Theoretical Tryptic Digest Map of Barstar with 0 Missed Cleavages Showing* $[M + 1H]^{1+}$ *and* $[M + 2H]^{2+}$

Peptide no.	Sequence	$[M + 1H]^{1+}$ (*m/z*)	$[M + 2H]^{2+}$ (*m/z*)	Observed ions
T1	MK	278.15	139.58	—
T2	K	147.11	74.06	—
T3	AVINGEQIR	999.56	500.28	500.28, 999.56
T4	SISDLHQTLK	1141.62	571.31	571.31
T5	K	147.11	74.06	—
T6	ELALPEYYGENDALWD CLTGWVEYPLVLEWR	3858.36	1929.69	—
T7	QFEQSK	766.37	383.69	766.37
T8	QLTENGAESVLQVFR	1690.88	845.94	845.94
T9	EAK	347.19	174.1	—
T10	AEGCDITIILS	1134.57	567.79	—

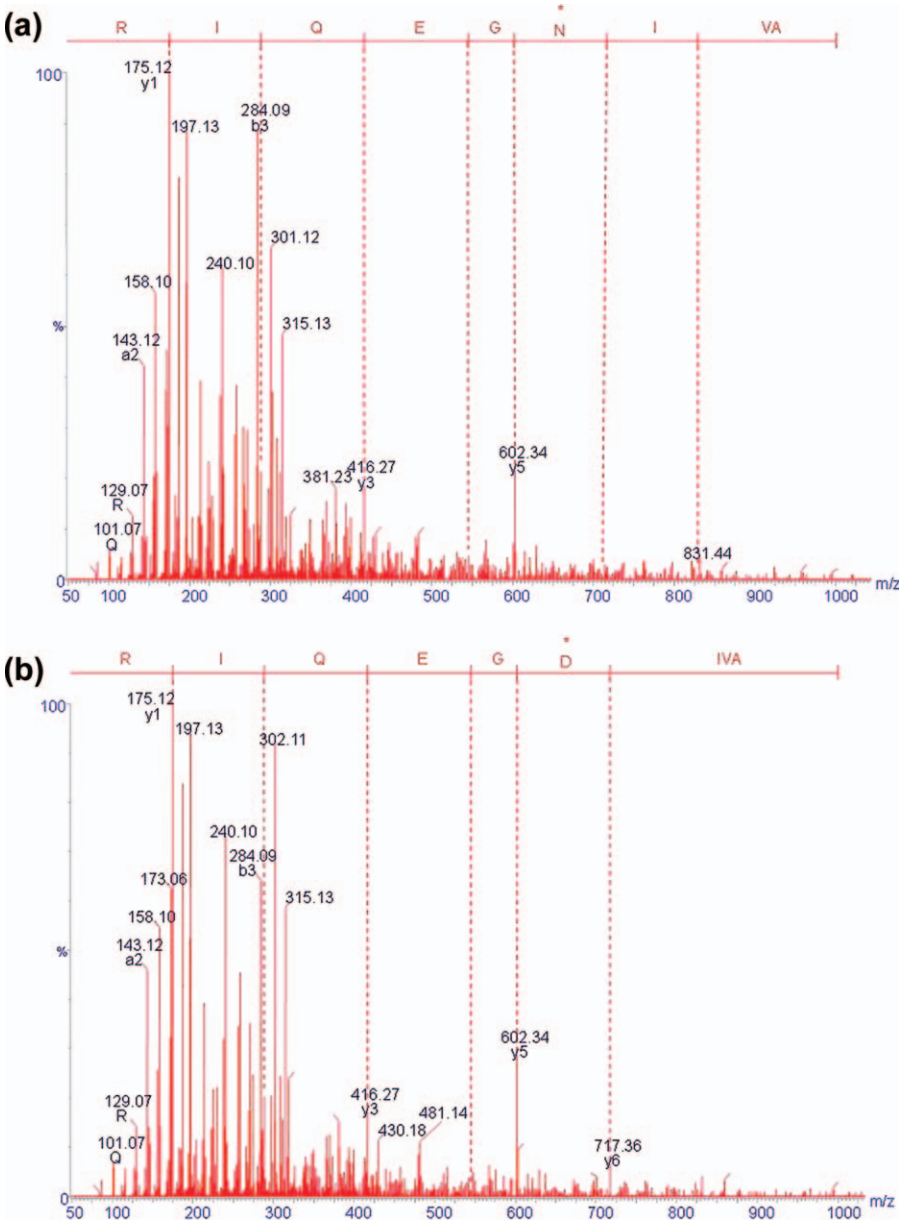

Figure 4. MS/MS of peptide T3 showing the site of modification. The spectra obtained after fragmentation were deconvoluted using MaxEnt 3 and submitted to MassSeq of the BioLynx application manager within MassLynx. Panel (a) indicates the "y" ion series for peptide T3 4AVINGEQIR12 after 0 h of incubation at pH 12.5. (b) Mass Lynx's MassSeq output of "y" ion series for peptide T3 after 5 h of incubation at pH 12.5. The sequence obtained is 4AVIDGEQIR12. * indicates the deamidated site. [Color figure can be viewed in the online issue, which is available at wileyonlinelibrary.com.]

mass of 1 Da each. Figure 3(d) shows the isotopic pattern of a control peptide T4–5 (645.36 *m/z*, 2^+), whose mass did not change when the protein was incubated at pH 12.5 for different time points under study.

Sequencing of the peptides reveals the sites of deamidation

To obtain the sequence of peptide T3 and peptide T8, tandem mass spectrometry (MS/MS) experiments were performed. Figure 4(a) shows the MS/MS spectrum of peptide T3 at 0 h incubation at pH 12.5. The observed ions are of the "y" ion series. The sequence of peptide T3 is deduced to be 4AVINGEQIR12. Figure 4(b) shows the MS/MS spectrum of the peptide T3 after 5 h of incubation at pH 12.5. The sequence of the modified peptide T3 is found to be 4AVIDGEQIR12. Although singly charged (999.56 *m/z*) and doubly charged (500.28 *m/z*) ions were observed, the fragmentation pattern is better when 2^+ charge state is fragmented under collision-induced dissociation.[52]

Figure 5(a) shows the MS/MS spectrum of peptide T8 when barstar is incubated at pH 12.5 for 0 h. The amino acid sequence of the peptide T8 is deduced to be 62QLTENGAESVLQVFR76. Figure 5(b) shows the MS/MS spectrum of peptide T8 after

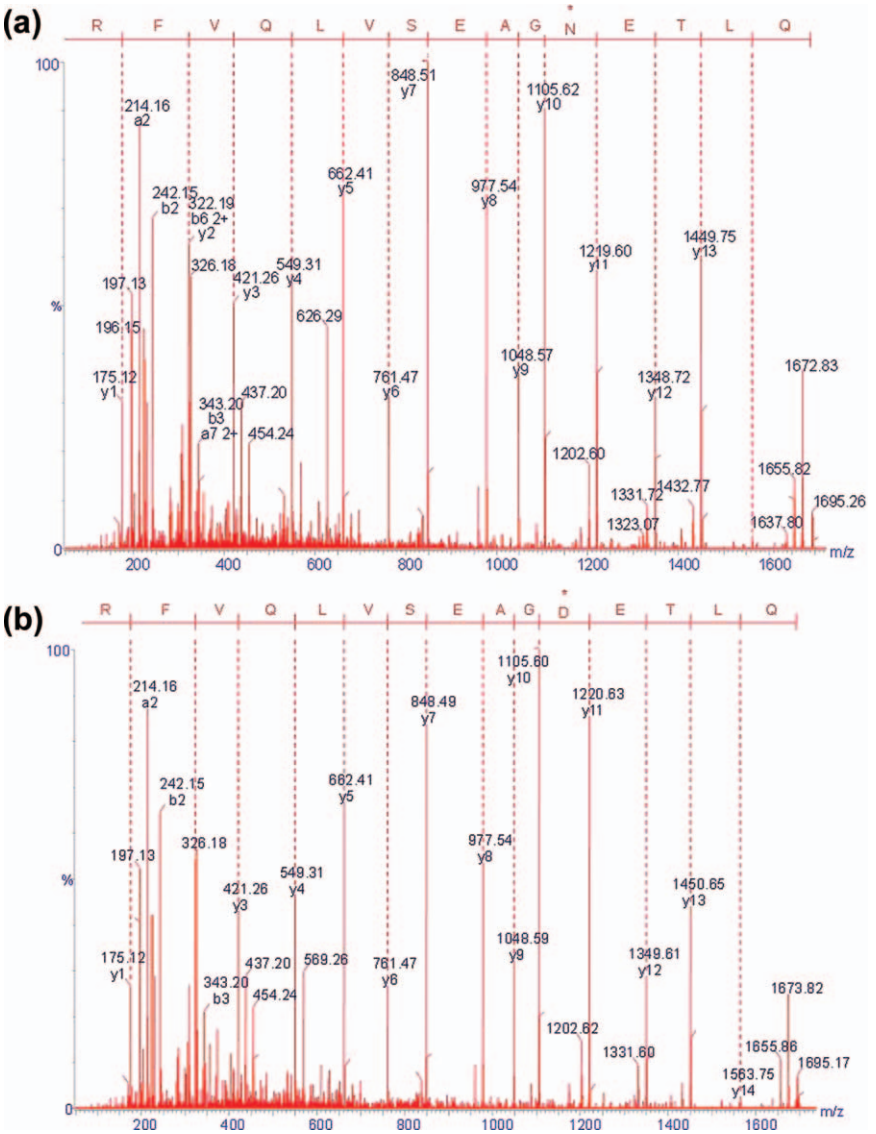

Figure 5. MS/MS of peptide T8 showing the site of modification. (a) MassLynx's MassSeq output of the "y" ion series for peptide T8 with the sequence 62QLTENGAESVLQVFR76 after 0 h of incubation at pH 12.5. (b) MassLynx's MassSeq output of "y" ion series for peptide T8 with the sequence 62QLTEDGAESVLQVFR76 after 5 h of incubation at pH 12.5. * indicates the deamidated site. [Color figure can be viewed in the online issue, which is available at wileyonlinelibrary.com.]

5 h of incubation at pH 12.5. The sequence obtained is 62QLTEDGAESVLQVFR76, which indicates the site of deamidation. All the observed ions in the mass spectra are of the "y" ion series.

Top-down sequencing of barstar confirms the sites of deamidation

A large peptide, T6 (1929.69 *m/z* 2^+), which has a potential deamidation site, N34, has not been observed by conventional bottom-up approach. Hence, top down sequencing, an approach to fragment an intact protein in MS, was performed. The most intense charge state of the protein, $[M+8H]^{8+}$, was fragmented inside MS and the product ions thus obtained were multiply charged ranging from 1^+ to 7^+ (data not shown). Figure 6(a,b) clearly indicates that positions N7 and N66 were deamidated upon incubation of the protein at pH 12.5 for 5 h. Analysis of the fragmentation pattern of $[M+8H]^{8+}$ of barstar indicated that residue N34 did not undergo deamidation upon incubation of the protein at pH 12.5 for 5 h [Fig. 6(c)].

Biophysical characterization of the deamidated protein

Figure 7 compares the tertiary and secondary structures of WT and deamidated barstar. Barstar has three tryptophan residues, and changes in the fluorescence of tryptophan residues have been shown to be a sensitive indicator of the changes in hydrophobic packing and tertiary structure of the protein.[17,53,54] Figure 7(a) shows the fluorescence emission spectra of the native (N) and unfolded (U) states of the WT and deamidated barstar. The

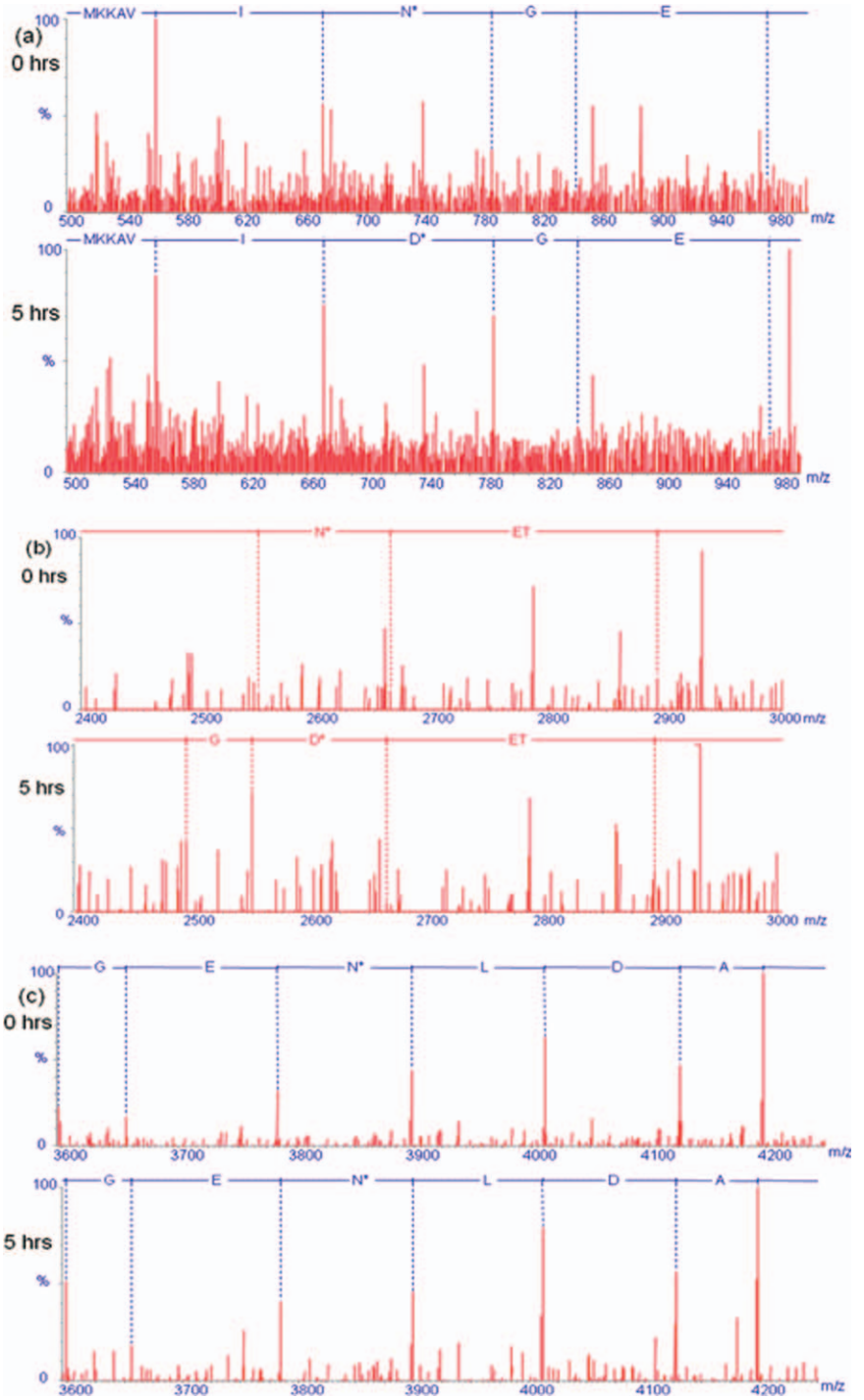

Figure 6. Confirming the sites of deamidation with top down sequencing. Max Ent 3 deconvoluted spectra of MS/MS of $[M+8H]^{8+}$ of intact barstar showing deamitated site in (a) position N7 with the sequence 1MKKAVINGE9 and (b) position N66 with the sequence 64TENG67, when the protein was incubated at pH 12.5 for 5 h. (c) Potential deamidated site N34 with the sequence 32GENLDA37 depicts the absence of deamidation of asparagine on incubation of the protein at pH 12.5 for 5 h. The sequence is of "b" ion series for positions N7 and N34. The sequence is of "y" ion series for position N66. * indicates site of deamidation. [Color figure can be viewed in the online issue, which is available at wileyonlinelibrary.com.]

emission maximum for both WT and deamidated barstar in the N state is at 334 nm. The U state of both the WT and deamidated proteins exhibits a large red shift with maximum emission occurring at 356 nm, which indicates that all of the tryptophan residues are fully exposed. The overlapping fluorescence emission spectra indicate that WT and deamidated barstar have the same tertiary structure.

The far-UV circular dichroism (CD) signal of a protein is a sensitive measure of its optically active secondary structure.[55] Figure 7(b) compares the far-UV CD spectra of the N and the U states of WT and

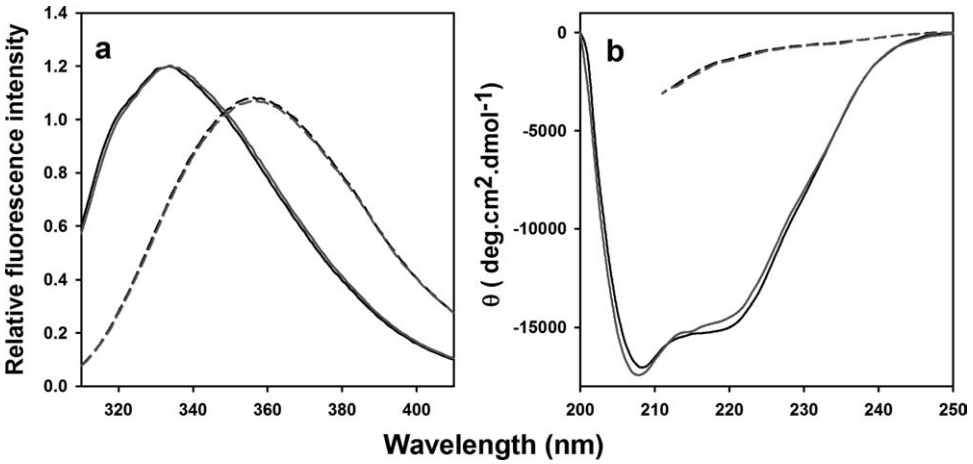

Figure 7. The tertiary and secondary structures of WT and deamidated barstar are similar. Panel (a) shows the fluorescence emission spectra of the WT (black lines) and deamidated (gray lines) proteins at pH 8.0 in 0*M* (solid lines) and 7*M* (dashed lines) urea, respectively, upon excitation at 295 nm. Panel (b) shows the far-UV CD spectra of the WT (black lines) and deamidated (gray lines) proteins at pH 8.0 in 0*M* (solid lines) and 7*M* (dashed lines) urea, respectively.

deamidated barstar. The mean residue ellipticities of WT barstar at 220 nm are $-15{,}000$ deg cm^2 dmol^{-1} in the N state and -1350 deg cm^2 dmol^{-1} in the U state. In comparison, the mean residue ellipticities of deamidated barstar at 220 nm are $-14{,}490$ deg cm^2 dmol^{-1} in the N state and -1430 deg cm^2 dmol^{-1} in the U state. These results suggest that the far-UV CD spectra of WT and deamidated barstar are the same (within the error of the measurements) and that the secondary structure of barstar is not perturbed upon deamidation. Deamidated barstar also retains the functional activity of WT barstar, that is, inhibition of the bacterial ribonuclease, barnase (data not shown).

The results presented above indicate that deamidated barstar fully recovers the tertiary and secondary structures and function of WT barstar, when brought back under native conditions. This is an important finding as for many proteins, including horse heart cytochrome *c* and βA3-crystallin, deamidation alters the biological activity and structure.[25,30,33,56]

Deamidation stabilizes an equilibrium intermediate during unfolding of barstar

To understand the effect of deamidation on the folding of barstar, equilibrium unfolding studies were carried out using fluorescence and far-UV CD as the probes. Figure 8 shows the equilibrium unfolding transitions of WT and deamidated barstar as monitored by changes in tryptophan fluorescence (a probe for changes in tertiary structure) and far-UV CD (a probe for hydrogen-bonded secondary structure). Figure 8(a) shows that both the tertiary structure and secondary structure of WT barstar are half unfolded at $3.44 \pm 0.02M$ of urea. The observation that dissolution of both the secondary and the tertiary structures occur together indicates that WT barstar unfolds in an N $\leftrightharpoons$ U two-state manner. Figure 8(b) shows that the tertiary structure of deamidated barstar is half unfolded at $2.51M$ of urea and the secondary structure is half unfolded at $3.12M$ of urea. The unfolding transitions of deamidated barstar, like those of WT barstar, are found to be completely reversible. The observation that the midpoints of the unfolding transitions of deamidated barstar are different when determined using different optical probes suggests that the unfolding of deamidated barstar does not follow a two-state N $\leftrightharpoons$ U model. The observation that deamidated barstar loses tertiary structure before the loss of secondary structure during its unfolding transition indicates that at least one equilibrium intermediate, with disrupted tertiary structure but intact secondary structure, is populated during its unfolding.

Discussion

Barstar gets deamidated at only two sites (N7 and N66) out of nine possible sites of deamidation (Scheme 1). The different factors that influence the deamidation reaction in proteins are the solvent accessibility of the asparagine, glutamine, and surrounding amino acid residues, the local amino acid sequence, and exposure to alkaline pH. Asparagine residues have been shown to be more prone to deamidation than glutamine residues,[58] as also observed in this study. Apart from the solvent accessibility, asparagine deamidation is also affected by the secondary and tertiary structures of the protein. In the case of ribonuclease A, although asparagine 67 residue is exposed to the solvent, a local β-turn conformation results in a structural constraint that appeared to protect the asparagine residue from deamidation.[59] In a study aimed at understanding the effect of the α-helical secondary structure on the

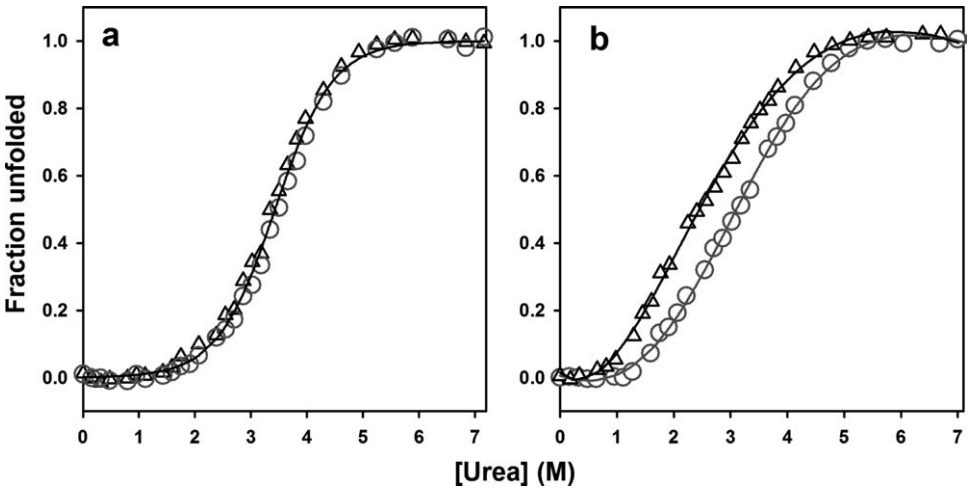

Figure 8. Deamidation populates an intermediate during the equilibrium unfolding of barstar. (a) WT and (b) deamidated barstar. In both panels, the black triangles show the equilibrium unfolding transition of the protein at pH 8.0, as monitored by a change in fluorescence at 320 nm, upon excitation at 295 nm, and the gray circles show the equilibrium unfolding transition of the protein as monitored by a change in the CD signal at 222 nm. The fraction of the unfolded protein is plotted against the concentrations of urea. The continuous black line through the data in panel (a) represents a nonlinear least-squares fit to a two-state N $\leftrightharpoons$ U model[57] to the average of the CD and fluorescence values. The continuous black and gray lines through the data in panel (b) represent a nonlinear least-squares fit to a two-state N $\leftrightharpoons$ U model.[57] The parameters associated with the two-state fits are described below. The midpoint of unfolding, C_m, is 3.44*M* urea for WT barstar and 3.12*M* (CD) and 2.51*M* (fluorescence) urea for deamidated barstar, respectively. The slope of the equilibrium unfolding transition, *m*-value, is 1.15 kcal mol^{-1} M^{-1} for WT barstar and 0.88 kcal mol^{-1} M^{-1} (CD) and 0.85 kcal mol^{-1} M^{-1} (fluorescence) for deamidated barstar, respectively. The free energy of unfolding, ΔG, is 4.0 kcal mol^{-1} for WT barstar and 2.7 kcal mol^{-1} (CD) and 2.1 kcal mol^{-1} (fluorescence) for deamidated barstar, respectively.

deamidation of asparagine residues, deamidation was seen to occur only in nonhelical populations.[60]

The solvent accessibilities of all the asparagine and glutamine residues in barstar, as predicted from its NMR structure,[61] are tabulated in Table II. There are three N residues in barstar, N7, N34, and N66. N66 is maximally exposed to solvent and is located in an unstructured loop connecting the third and the fourth helix in the protein, and not surprisingly it is one of the sites that get deamidated when the protein is kept at alkaline pH for a few hours. Of the three asparagine residues, N7 is least exposed to solvent (~30%) and is located in a partially structured region of the protein (at the end of the first β-strand). However, it gets deamidated in preference to N34, which is ~50% exposed to solvent and is positioned in an unstructured loop connecting the first and the second helix. Clearly, factors other than solvent accessibility and the conformation of the protein play a role in the deamidation reactions of barstar.

It is interesting to note that the residue immediately C terminal to both the deamidation sites (N7 and N66) in barstar is glycine. In the deamidation reaction of asparagine residues in proteins, the nitrogen atom of the backbone amide of the residue immediately C terminal to the asparagine attacks the nucleophilic carbonyl of the asparagine side chain.[39,58] A cyclic succinimide intermediate is produced, which is hydrolyzed to a mixture of aspartate and isoaspartate residues, having the same mass. The formation of cyclic succinimide by the attack of the backbone amide is the rate-limiting step for the deamidation reaction and is influenced by steric effects. Its formation is favored if the side chain of the residue C terminal to the asparagine residue is small in size.[32,58] Glycine, having the smallest side chain, offers the least steric hindrance. Hence, barstar gets deamidated preferentially at those asparagine sites whose immediate C-terminal residue is glycine.

Table II. *Whole-Residue Solvent Accessibilities of All the Asparagine and Glutamine Residues (the Possible Sites of Deamidation) in Barstar as Predicted from the NMR Structure*[60]

Amino acid residue	Percentage solvent accessibility (%)
N7	**~30**
Q10	~65–70
Q19	~50
N34	~50
Q56	~30
Q59	~60
Q62	~30
N66	**~80**
Q73	~10

Deamidated residues are shown in bold letters.

For both the peptides T3 (containing N7) and T8 (containing N66), the monoisotopic peak intensities are reduced by similar amounts after 2 h of incubation at pH 12.5 [Fig. 3(b,c)]. This observation suggests that the rates of deamidation at both the sites, N7 and N66, may be similar. Hence, it was not possible to determine whether one or both of the deamidation reactions are responsible for the stabilization of the intermediate. Work is in progress in the laboratory to prepare mutant proteins with single and double Asn → Asp mutations, using site-directed mutagenesis. Equilibrium unfolding experiments on these mutant proteins are expected to resolve this issue in future.

During the deamidation reaction, neutral amide groups of both the asparagine residues get modified to aspartic acid residues, which must be present as negatively charged aspartate residues at pH 8.0. This increase in negative charge on the protein may increase the electrostatic repulsion between the negatively charged residues resulting in tertiary structure disruption preceding secondary structure disruption. Changes in the electrostatics of the protein chain by changes in the pH of the solvent have been shown to stabilize folding intermediates and to cause a switch from apparent two-state folding to three-state folding in the case of many proteins, including protein G,[62] immunity proteins,[63] hisactophilin,[64] and thioredoxin.[16]

The slope of equilibrium unfolding transition (equilibrium *m*-value) for the deamidated barstar is 0.88 kcal mol^{-1} M^{-1} (CD) and 0.85 kcal mol^{-1} M^{-1} (fluorescence) and for the WT barstar is 1.15 kcal mol^{-1} M^{-1}, respectively (Fig. 8). This result suggests that the stabilization of the equilibrium intermediate decreases the slope of equilibrium unfolding transition for the deamidated barstar. Deamidation of asparagine has been reported to give a mixture of aspartic and isoaspartic acid.[35,39,43,58] It is possible that a minor fraction of barstar forms isoaspartic acid, in addition to aspartic acid, upon deamidation, and this heterogeneity in population is responsible for some of the broadness of the equilibrium unfolding transition [Fig. 8(b)]. It is unlikely, however, that a major fraction of barstar forms isoaspartic acid because of the following reasons: (i) deamidation of asparagine to isoaspartic acid results in a serious perturbation to the protein backbone and the secondary structure of the protein is compromised.[35,39] Deamidated barstar, however, has the same secondary structure as the WT barstar as measured using far-UV CD [Fig. 7(b)] and also retains the functional activity of the protein (see above). (ii) Peptides with isoaspartyl residues are reported to elute earlier than with aspartyl residues in reversed-phase chromatography.[65] The extracted ion chromatogram of the peptide T3 and T8 of barstar containing N7 and N66, respectively, resulted, however, in only one peak indicating only one form of deamidated asparagine (data not shown). Future equilibrium unfolding studies on the mutant variants of barstar described above (containing single and double Asn → Asp mutations) would be helpful in determining what fraction of barstar, if any, forms isoaspartic acid upon deamidation.

Proteins fold along well-defined pathways, which involve partly folded intermediate structures.[12–14,66] The study and structural characterization of intermediate structures that are partly folded is essential to understand the complex protein-folding reactions. The observation of cooperative two-state equilibrium unfolding transitions for many small proteins is usually interpreted as the absence of intermediate structures during folding.[67] However, intermediate structures will also not be detected at equilibrium if they are less stable than the fully unfolded and fully folded protein. Folding intermediates can be populated at equilibrium if they are sufficiently stabilized with respect to either the U state or the N state or by the sufficient destabilization of either the N or U state with respect to the intermediate state. Such stabilization can be achieved in many ways, which include changes in protein sequence by mutation and changes in protein environment such as pH and solvent.[16,17,68]

Deamidation is a common covalent modification that may occur in proteins during storage in solution. In this study, it was observed that deamidation of the protein sequence at two residues alters the equilibrium unfolding mechanism of barstar from two state to apparently three state. Therefore, it is critical to identify deamidation in proteins used for folding studies.

Materials and Methods

All the solvents were of HPLC grade (Spectrochem). Glufibrinopeptide (SIGMA) was used as the calibrant. Chemicals [dithiothreitol (DTT), iodoacetamide (IAA), trypsin, formic acid (FA), sodium tetraborate, EDTA, and Tris] were from SIGMA. Water was purified using a MilliQ filtration system.

Protein purification

Wild-type (WT) barstar was purified as described previously.[53] Protein purity was checked by MS, using a QToF Ultima API mass spectrometer (Waters Corporation, Milford, MA), coupled with an ESI source. The mass determined for WT barstar was 10342.66 Da, which indicates that the N-terminal methionine residue remained uncleaved during the expression of this protein in *Escherichia coli* strain MM294. The concentration of the protein was determined by measuring the absorbance at 280 nm, using an extinction coefficient of 23,000 M^{-1} cm^{-1}.[53]

Sample preparation

Ten milligrams of barstar was dissolved in 1.0 mL of native buffer (50 m*M* Tris, 1.0 m*M* EDTA, and 1.0 m*M* DTT) at pH 8.0. The protein in the native buffer was diluted 10-fold in a high pH buffer containing 50 m*M* sodium tetraborate, 1.0 m*M* EDTA, and 1.0 m*M* DTT at pH 12.5 to facilitate the deamidation reaction. At different times of incubation of the protein (0, 2, and 5 h) in pH 12.5 buffer, 100 μL of the deamidated protein solution was diluted to 1.0 mL in the native buffer at pH 8.0 to quench the deamidation reaction. The resultant solution was desalted using a Sephadex G-25 high-trap desalting column on an AKTA-chromatography system and was analyzed by MS.

Mass spectrometry

MS experiments were carried out using ESI QToF Ultima (Waters Corporation, Milford, MA) using Z-spray ionization. The instrument is calibrated with MS/MS of GFP in the mass range 50–2000 *m/z*. The instrument was set at a resolution of 10,000 (full width at half maximum, FWHM) for all experiments and at 20,000 (FWHM) to study the changes in the isotopic pattern of $[M+8H]^{8+}$ of barstar due to deamidation. The optimum QToF parameters used to obtain the intact mass data were as follows: capillary voltage 3.5 kV, cone voltage 70 V, source temperature 80°C, desolvation temperature 200°C, and collision energy (CE) 10eV. Data were acquired for 3 min with a scan time of 1.0 s and interscan delay of 0.1 s. The intact mass spectra shown are raw data with minimal smoothening. The spectra were deconvoluted to the zero charge state using Max Ent 1, a deconvolution software available within MassLynx 4.0.

For top down sequencing, intact protein was directly infused into MS at a concentration of 5 pmol μL^{-1}. The most intense charge state of the protein, $[M+8H]^{8+}$, was selected in the first quadrupole and fragmented in the collision cell with a CE of 30–40 eV, whereas the source parameters were the same as mentioned above. Argon gas was used in the collision cell to obtain MS/MS data. MS/MS spectra thus obtained were processed using Max Ent 3, a deconvolution software for peptides (Ensemble 1, Iterations 50, auto peak width determination) within MassLynx 4.0. The deconvoluted spectra were then imported into Mass Seq (MassLynx's denovo sequencing tool) to obtain a sequence tag. Manual deconvolutions were done to recheck the analysis.

CapLC ESI QToF MS

Deamidated barstar at different time points (0, 2, and 5 h) was reduced with DTT, alkylated with IAA, and digested overnight with trypsin at 37°C according to the protocol of Kinter and Sherman.[69] The digested samples at different time points were injected through CapLC ESI QToF MS (Waters Corporation, Milford, MA). Solvent A is 90:10 (water: acetonitrile) in 0.1% FA. Solvent B is 90:10 (acetonitrile:water) in 0.1% FA. The gradient used to separate the peptides was 5–50% B in 30 min. The sample was trapped onto the trap column (Symmetry C18, 5 μm, 0.18 mm × 23.5 mm) to concentrate and cleanup the sample. A gradient was then applied to separate the peptides in the analytical column (Atlantis dC18, 5 μm, 300 μm, and 15 cm) at a flow rate of 5 $\mu L\ min^{-1}$. CapLC was directly connected to ESI QToF MS. The optimum QToF parameters used to obtain the CapLC data were as follows: capillary voltage 3.5 kV, cone voltage 70 V, source temperature 80°C, and CE 10 eV. Data-dependent analysis method was used to acquire the data, which gave MS and MS/MS of two peptides in a single run. For MS/MS data, the CE default profile was set, which was based on the charge state and mass of the peptides.

CapLC ESIMS data were minimally smoothened and no further processing was performed. The MS/MS spectra were deconvoluted using Max Ent 3 (Ensemble 1, iterations 50, auto peak width determination), an application manager within MassLynx 4.0. The deconvoluted spectra were submitted to Mass Seq (MassLynx's denovo sequencing tool) to obtain a sequence tag. The sequence tag thus obtained was compared with the theoretical sequence of barstar (Scheme 1).

Fluorescence and far-UV CD spectrum

The fluorescence spectra were collected on a Spex Fluoromax 3 spectrofluorometer. The excitation wavelength was set to 295 nm. Emission spectra were recorded in a cuvette of 1.0 cm path length, with excitation slit width set at 0.5 nm and emission slit width set at 10 nm. The protein concentration used was ~5 μ*M*. All the spectra were recorded at pH 8.0 and at 25°C.

The far-UV CD spectra were collected on a Jasco J 720 spectropolarimeter. Secondary structure was monitored in the wavelength range of 200–250 nm using a cuvette cell of 0.1 cm path length. A spectral bandwidth of 2 nm and a time constant of 1.0 s were used, and each spectrum was recorded as an average of 20 scans. The protein concentration used was ~20 μ*M*. All the spectra were recorded at pH 8.0 and at 25°C.

Equilibrium unfolding experiments

Equilibrium unfolding of the WT and the deamidated barstar was monitored using fluorescence and far-UV CD. The protein was incubated at different concentrations of urea ranging from 0 to 8.0*M* for 6 h, and the equilibrium fluorescence signals were measured on the Spex Fluoromax 3 spectrofluoro-

meter in a cuvette of 1.0 cm path length. Sample excitation was carried out at 295 nm with the excitation slit width set at 0.5 nm, and emission was monitored at 320 nm with the emission slit width set at 10 nm.

Equilibrium far UV-CD signals were monitored for the same samples, which were used for fluorescence experiments, on the Jasco J 720 spectropolarimeter in a cuvette of 1.0 cm path length. The protein concentration used was $\sim$10 μM. All the experiments were performed at pH 8.0 and at 25°C. Equilibrium unfolding transitions monitored by either fluorescence or CD were analyzed according to a two-state, N $\leftrightharpoons$ U model.[57] The purpose of carrying out two-state analysis of the deamidated protein is only to show that the fluorescence and CD-monitored transitions are not coincident, on the basis of the C_m values determined from two-state analysis. For a proper analysis of the equilibrium unfolding data for the deamidated protein, three-state analysis as described earlier[17] would have to be carried out. This has not been done because the purpose of this study is merely to demonstrate that equilibrium intermediate is populated upon deamidation and not to determine the energetics of unfolding of the deamidated protein.

Acknowledgments

All mass spectra were collected at the Mass Spectrometry Facility at the National Centre for Biological Sciences, Bangalore. JBU is a recipient of a JC Bose National Fellowship from the Government of India. SKJ acknowledges Council of Scientific and Industrial Research (CSIR), India, for a Shyama Prasad Mukherjee Fellowship.

References

1. Mirsky AE, Pauling L (1936) On the structure of native, denatured, and coagulated proteins. Proc Natl Acad Sci USA 22:439–447.
2. Anson ML (1939) The denaturation of proteins by detergents and bile salts. Science 90:256–257.
3. Levinthal C (1968) Are there pathways for protein folding? J Chim Phys 65:44–45.
4. Levinthal C, How to fold graciously. In: DeBrunner JTP, Munck E, Eds. (1969) Mossbauer spectroscopy in biological systems: Proceedings of a Meeting held at Allerton House, Monticello, Illinois. Urbana: University of Illinois Press, pp 22–24.
5. Anfinsen CB (1973) Principles that govern the folding of protein chains. Science 181:223–230.
6. Baldwin RL (2008) The search for folding intermediates and the mechanism of protein folding. Annu Rev Biophys 37:1–21.
7. Udgaonkar JB (2008) Multiple routes and structural heterogeneity in protein folding. Annu Rev Biophys 37: 489–510.
8. Jackson SE (1998) How do small single-domain proteins fold? Fold Des 3:R81–R91.
9. Jha SK, Udgaonkar JB (2010) Free energy barriers in protein folding and unfolding. Curr Sci 99:457–475.
10. Ptitsyn OB (1973) Stages in the mechanism of self-organization of protein molecules. Dokl Akad Nauk SSSR 210:1213–1215.
11. Karplus M, Weaver DL (1976) Protein-folding dynamics. Nature 260:404–406.
12. Kim PS, Baldwin RL (1982) Specific intermediates in the folding reactions of small proteins and the mechanism of protein folding. Annu Rev Biochem 51: 459–489.
13. Udgaonkar JB, Baldwin RL (1988) NMR evidence for an early framework intermediate on the folding pathway of ribonuclease A. Nature 335:694–699.
14. Karplus M, Weaver DL (1994) Protein folding dynamics: the diffusion–collision model and experimental data. Protein Sci 3:650–668.
15. Jackson SE, Fersht AR (1991) Folding of chymotrypsin inhibitor-2. I. Evidence for a two-state transition. Biochemistry 30:10428–10435.
16. Wani AH, Udgaonkar JB (2006) HX-ESI-MS and optical studies of the unfolding of thioredoxin indicate stabilization of a partially unfolded, aggregation-competent intermediate at low pH. Biochemistry 45: 11226–11238.
17. Nath U, Udgaonkar JB (1995) Perturbation of a tertiary hydrogen bond in barstar by mutagenesis of the sole His residue to Gln leads to accumulation of at least one equilibrium folding intermediate. Biochemistry 34:1702–1713.
18. Inaba K, Kobayashi N, Fersht AR (2000) Conversion of two-state to multi-state folding kinetics on fusion of two protein foldons. J Mol Biol 302:219–233.
19. Spudich GM, Miller EJ, Marqusee S (2004) Destabilization of the Escherichia coli RNase H kinetic intermediate: switching between a two-state and three-state folding mechanism. J Mol Biol 335:609–618.
20. Korzhnev DM, Salvatella X, Vendruscolo M, Di Nardo AA, Davidson AR, Dobson CM, Kay LE (2004) Low-populated folding intermediates of Fyn SH3 characterized by relaxation dispersion NMR. Nature 430: 586–590.
21. Wani AH, Udgaonkar JB (2009) Revealing a concealed intermediate that forms after the rate-limiting step of refolding of the SH3 domain of PI3 kinase. J Mol Biol 387:348–362.
22. Wani AH, Udgaonkar JB (2009) Native state dynamics drive the unfolding of the SH3 domain of PI3 kinase at high denaturant concentration. Proc Natl Acad Sci USA 106:20711–20716.
23. Jha SK, Udgaonkar JB (2009) Direct evidence for a dry molten globule intermediate during the unfolding of a small protein. Proc Natl Acad Sci USA 106: 12289–12294.
24. Jha SK, Dhar D, Krishnamoorthy G, Udgaonkar JB (2009) Continuous dissolution of structure during the unfolding of a small protein. Proc Natl Acad Sci USA 106:11113–11118.
25. Takata T, Oxford JT, Brandon TR, Lampi KJ (2007) Deamidation alters the structure and decreases the stability of human lens βA3-crystallin. Biochemistry 46:8861–8871.
26. Moss CX, Matthews SP, Lamont DJ, Watts C (2005) Asparagine deamidation perturbs antigen presentation on class II major histocompatibility complex molecules. J Biol Chem 280:18498–18503.
27. Chen W, Ede NJ, Jackson DC, McCluskey J, Purcell AW (1996) CTL recognition of an altered peptide associated with asparagine bond rearrangement. Implications for immunity and vaccine design. J Immunol 157: 1000–1005.

28. Flatmark T, Sletten K (1968) Multiple forms of cytochrome c in the rat. J Biol Chem 243:1623–1629.
29. McKerrow JH, Robinson AB (1974) Primary sequence dependence of the deamidation of rabbit muscle aldolase. Science 183:85.
30. Robinson AB, McKerrow JH, Cary P (1970) Controlled deamidation of peptides and proteins: an experimental hazard and a possible biological timer. Proc Natl Acad Sci USA 66:753–757.
31. Takemoto L, Boyle D (2000) Specific glutamine and asparagine residues of γ-S crystallin are resistant to in vivo deamidation. J Biol Chem 275:26109–26112.
32. Robinson NE, Robinson AB (2001) Molecular clocks. Proc Natl Acad Sci USA 98:944–949.
33. Flatmark T (1967) Multiple molecular forms of bovine heart cytochrome c. V. A comparative study of their physicochemical properties and their reactions in biological systems. J Biol Chem 242:2454–2459.
34. Venkatesh YP, Vithayathyl PJ (1984) Isolation and characterization of monodeamidated derivatives of bovine pancreatic ribonuclease A. Int J Pept Res 23: 494–505.
35. Di Donato A, Ciardiello MA, de Nigris M, Piccoli RL, Mazzarella L, D'Alessio G (1993) Selective deamidation of ribonuclease A. Isolation and characterization of the resulting isoaspartyl and aspartyl derivatives. J Biol Chem 268:4745–4751.
36. Solstad T, Carvalho RN, Andersen OA, Waidelich D, Flatmark T (2003) Deamidation of labile asparagine residues in the autoregulatory sequence of human phenylalanine hydroxylase. Eur J Biochem 270:929–938.
37. Thannhauser T, Scheraga HA (1985) Reversible blocking of half-cysteine residues of proteins and an irreversible specific deamidation of asparagine-67 of S-sulforibonuclease under mild conditions. Biochemistry 24:7681–7688.
38. Solstad T, Flatmark T (2000) Microheterogeneity of recombinant human phenylalanine hydroxylase as a result of nonenzymatic deamidations of labile amide containing amino acid. Eur J Biochem 267:6302–6310.
39. Chelius D, Rehder DS, Bondarenko PV (2005) Identification and characterization of deamidation sites in the conserved regions of human immunoglobulin gamma antibodies. Anal Chem 77:6004–6011.
40. Catanzano F, Graziano G, Capasso S, Barone G (1997) Thermodynamic analysis of the effect of selective monodeamidation at asparagine 67 in ribonuclease A. Protein Sci 6:1682–1693.
41. Orru S, Vitagliano L, Esposito L, Mazzarella L, Marino G, Ruoppolo M (2000) Effect of deamidation on folding of ribonuclease A. Protein Sci 9:2577–2582.
42. Zabrouskov V, Han X, Welker E, Zhai H, Lin C, van Wijk KJ, Scheraga HA, McLafferty FW (2006) Stepwise deamidation of ribonuclease A at five sites determined by top down mass spectrometry. Biochemistry 45: 987–992.
43. Lehmann WD, Schlosser A, Erben G, Pipkorn R, Bossemeyer D, Kinzel V (2000) Analysis of isoaspartate in peptides by electrospray tandem mass spectrometry. Protein Sci 9:2260–2268.
44. Robinson NE, Zabrouskov V, Zhang J, Lampi KJ, Robinson AB (2006) Measurement of deamidation of intact proteins by isotopic envelope and mass defect with ion cyclotron resonance Fourier transform mass spectrometry. Rapid Commun Mass Spectrom 20: 3535–3541.
45. Schreiber G, Fersht AR (1993) The refolding of cis- and trans-peptidylprolyl isomers of barstar. Biochemistry 32:11195–11203.
46. Shastry MC, Udgaonkar JB (1995) The folding mechanism of barstar: evidence for multiple pathways and multiple intermediates. J Mol Biol 247:1013–1027.
47. Sridevi K, Udgaonkar JB (2003) Surface expansion is independent of and occurs faster than core solvation during the unfolding of barstar. Biochemistry 42: 1551–1563.
48. Jha SK, Udgaonkar JB (2007) Exploring the cooperativity of the fast folding reaction of a small protein using pulsed thiol labeling and mass spectrometry. J Biol Chem 282:37479–37491.
49. Schöppe A, Hinz HJ, Agashe VR, Ramachandran S, Udgaonkar JB (1997) DSC studies of the conformational stability of barstar wild-type. Protein Sci 6: 2196–2202.
50. Lakshmikanth GS, Sridevi K, Krishnamoorthy G, Udgaonkar JB (2001) Structure is lost incrementally during the unfolding of barstar. Nat Struct Biol 8:799–804.
51. Deepalakshmi PD (2009) Characterization of recombinant protein mutants by top down sequencing using quadrupole time of flight mass spectrometry. Eur J Mass Spectrom 15:641–649.
52. Huang Y, Triscari JM, Tseng GC, Pasa-Tolic L, Lipton MS, Smith RD, Wysocki VH (2005) Statistical characterization of the charge state and residue dependence of low-energy CID peptide dissociation patterns. Anal Chem 77:5800–5813.
53. Khurana R, Udgaonkar JB (1994) Equilibrium unfolding studies of barstar: evidence for an alternative conformation which resembles a molten globule. Biochemistry 33:106–115.
54. Agashe VR, Shastry MC, Udgaonkar JB (1995) Initial hydrophobic collapse in the folding of barstar. Nature 377:754–757.
55. Kelly SM, Price NC (2000) The use of circular dichroism in the investigation of protein structure and function. Curr Protein Pept Sci 1:349–384.
56. Takata T, Woodbury LG, Lampi KJ (2009) Deamidation alters interactions of β-crystallins in hetero-oligomers. Mol Vis 15:241–249.
57. Agashe VR, Udgaonkar JB (1995) Thermodynamics of denaturation of barstar: evidence for cold denaturation and evaluation of the interaction with guanidine hydrochloride. Biochemistry 34:3286–3299.
58. Cournoyer JJ, Lin C, O'Connor PB (2006) Detecting deamidation products in proteins by electron capture dissociation. Anal Chem 78:1264–1271.
59. Wearne SJ, Creighton TE (1989) Effect of protein conformation on rate of deamidation: ribonuclease A. Proteins 5:8–12.
60. Kosky AA, Razzaq UO, Treuheit MJ, Brems DN (1999) The effects of α-helix on the stability of Asn residues: deamidation rates in peptides of varying helicity. Protein Sci 8:2519–2523.
61. Lubienski MJ, Bycroft M, Freund SM, Fersht AR (1994) Three-dimensional solution structure and 13C assignments of barstar using nuclear magnetic resonance spectroscopy. Biochemistry 33:8866–8877.
62. Park SH, Shastry MC, Roder H (1999) Folding dynamics of the B1 domain of protein G explored by ultra rapid mixing. Nat Struct Biol 6:943–947.
63. Gorski SA, Capaldi AP, Kleanthous C, Radford SE (2001) Acidic conditions stabilize intermediates populated during the folding of Im7 and Im9. J Mol Biol 312:849–863.
64. Houliston RS, Liu C, Singh LM, Meiering EM (2002) pH and urea dependence of amide hydrogen-deuterium exchange rates in the β-trefoil protein hisactophilin. Biochemistry 41:1182–1194.

65. Geiger T, Clarke S (1987) Deamidation and racemization at asparaginyl and aspartyl residues in peptides. J Biol Chem 262:785–794.
66. Jha SK, Dasgupta A, Malhotra P, Udgaonkar JB (2011) Identification of multiple folding pathways of monellin using pulsed thiol labeling and mass spectrometry. Biochemistry 50:3062–3074.
67. Privalov PL (1992) Protein folding. New York: WH Freeman & Co, p 83.
68. Connell KB, Horner GA, Marqusee S (2009) A single mutation at residue 25 populates the folding intermediate of E. coli RNase H and reveals a highly dynamic partially folded ensemble. J Mol Biol 391:461–470.
69. Kinter M, Sherman NE, The preparation of protein digests for mass spectrometric sequencing experiments. In: Desiderio DM, Nibbering NMM, Eds. (2000) Protein sequencing and identification using tandem mass spectrometry. New York: Wiley, pp 147–165.